Homo- and Heterojunction Dual-Band Detectors

A. G. Unil Perera, G. Ariyawansa, M. B. M. Rinzan,

M. Alevli, M. Strassburg, and N. Dietz

Department of Physics and Astronomy
Georgia State University

S. G. Matsik

NDP Optronics, Mableton, Georgia, 30126

A. Asghar and I. T. Ferguson

School of Electrical and Engineering, Georgia Institute of Technology, Atlanta, Georgia, 30332

H. Luo, A. Bezinger, and H. C. Liu

Institute for Microstructural Sciences, National Research Council, Ottawa K1A OR6, Canada

Supported by:
U. S. National Science Foundation (NSF) under grant ECS#0553051
U. S. Air Force under contract (SBIR) FA9453-05-M-0106

Colleagues and Collaborators

- Colleagues

N. Dietz and his group
S. Matsik
H. J. Peng
D. Esaev
M. Rinzan
A. Weerasekara
G. Ariyawansa
V. Jayaweera
R. Jayasinghe

- Collaborators

H. C. Liu	– NRC Canada
S. Krishna	– U. New Mexico
P. Bhattacharya	– U. Michigan
Y. Paltiel	– Soreq NRC Israel
V. Gavrilenko	– Nizhni Novgorod
B. Zvonkov	– Nizhni Novgorod
I. Ferguson	– Georgia Tech.
H. H. Tan	– Australian National Univ.
C. Jagadish	– Australian National Univ.

Outline

- Dual Band Detector Applications
- HIWIP (Homojunction) and HEIWIP (Heterojunction) Interfacial Workfunction Internal Photoemission Detectors
- Dual-Band Detection Mechanism
- Experimental Results
  - Si HIWIP Dual Band Detector
  - GaAs HIWIP Dual Band Detector
  - GaN/AlGaN HEIWIP Dual Band Detector
- Conclusion

Dual Band Detector Applications
Land Mine Detection

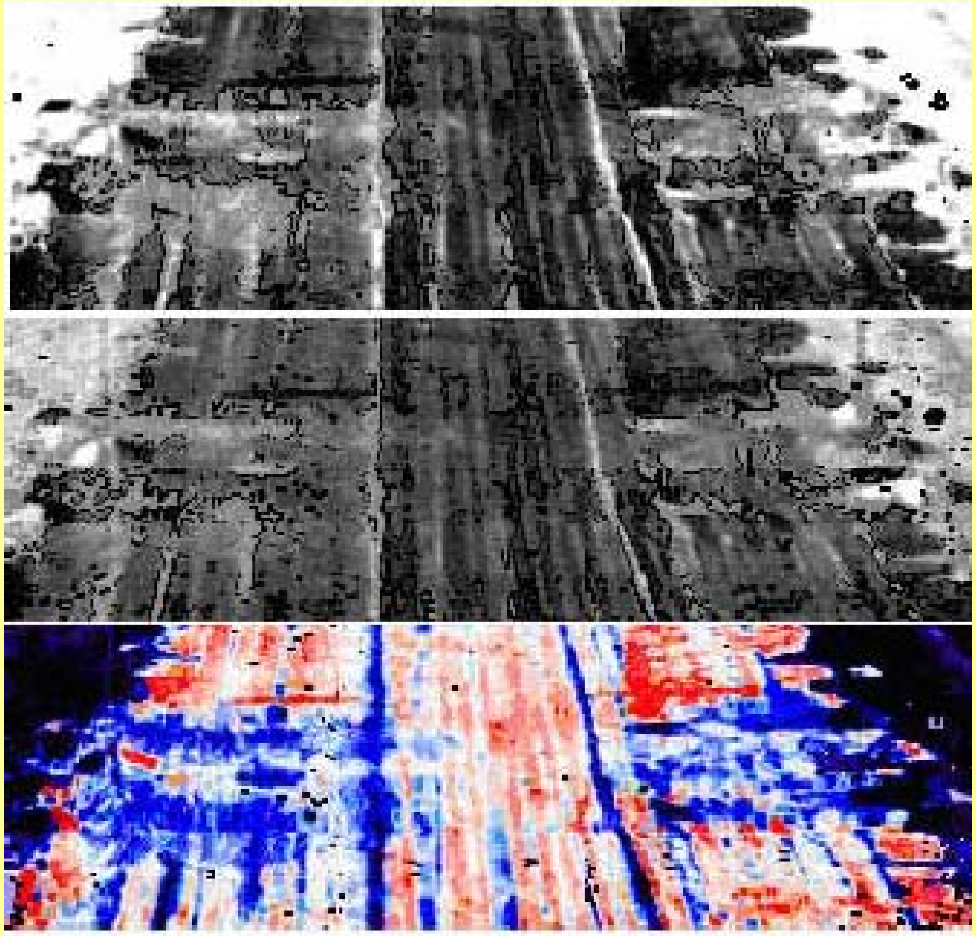

Image 1 taken with the 9 μm band

Disturbed soil is highly emissive

Image 2 taken with the 10.5 μm band

No or little effect of the disturbed soil

Fused Image =

Image 1- Image 2

Blue shows areas of disturbed soil indicative of buried mines

Infrared Phys. and Technol.(**44**) 427 (2003)

Dual Band Detector Applications

Horsehead Nebula

Visible | Near-infrared | Mid-infrared

UV/ IR dual band detectors >>

Fire and Flame detection: Different type of fires emit radiation from UV to IR with different intensities.

Hydrogen and coal flames have significant intensity variation in the emission spectrum in the UV and IR regions.

Horsehead Nebula: http://coolcosmos.ipac.caltech.edu/cosmic_classroom/ir_tutorial/irregions.htm

Internal Photoemission Detectors

Type I - $N_d < N_c$ ($E_C^{n+} > E_F$)

N_d : Doping of Emitter

N_c : Mott's critical concentration

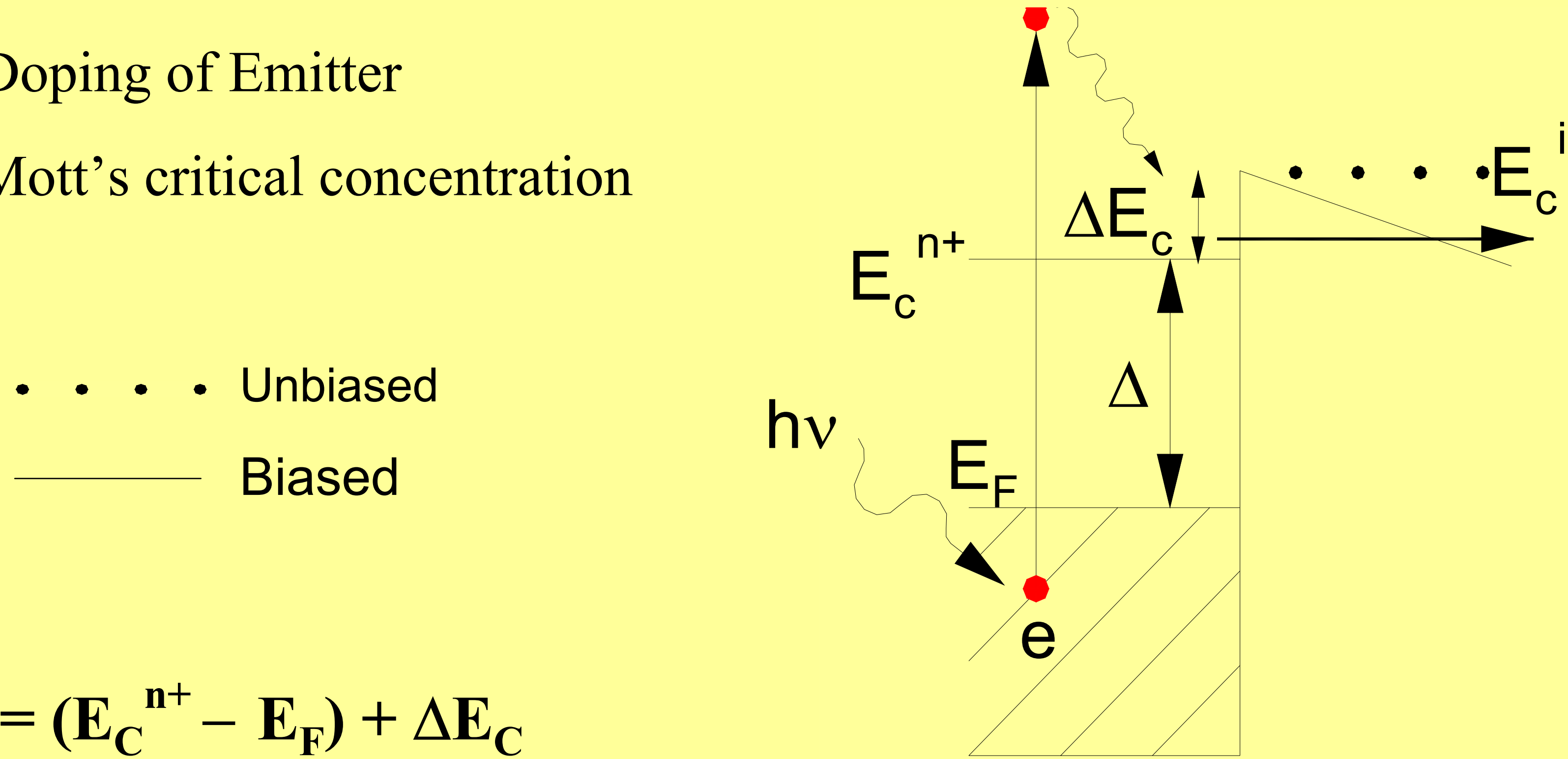

$$\Delta = (E_C^{n+} - E_F) + \Delta E_C$$

JAP (**77**) 915 (1995)

Type II - $N_c < N_d < N_0$ ($E_C^{n+} < E_F < E_C^{i}$)

N_d : Doping density in the Emitter/Absorber

N_c : Mott's critical concentration

N_0 : Critical concentration

$$\Delta = E_c^{i} - E_F$$

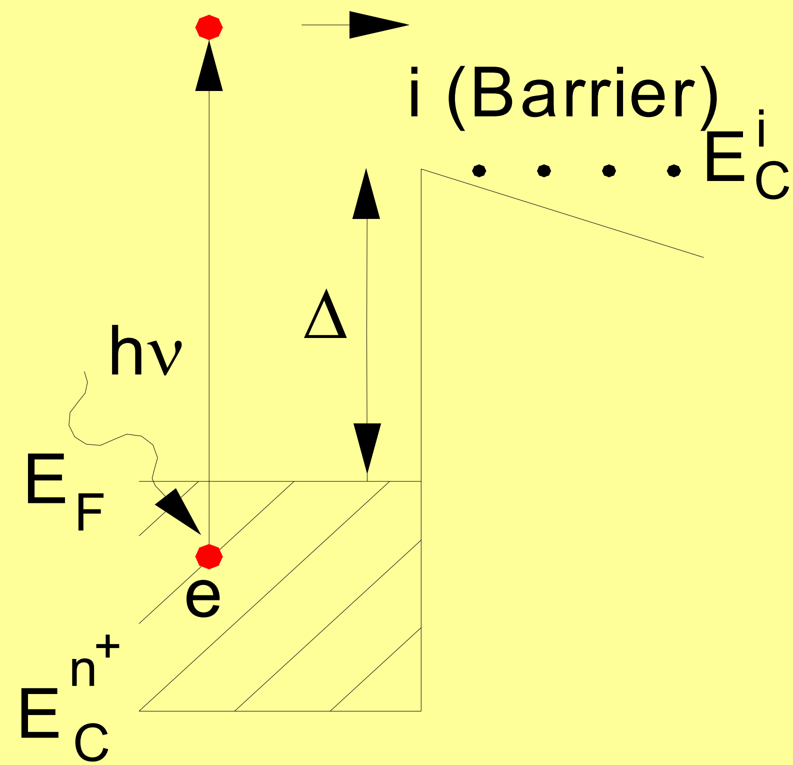

- Fermi level is above the conduction band edge of the emitter
- Emitter becomes semi-metallic
- Infrared absorption is due to free carriers

JAP (**77**) 915 (1995)

Type III - $N_d > N_0$ ($E_F > E_C^i$)

N_d : Doping concentration of the Emitter/ Absorber

N_0 : Critical concentration

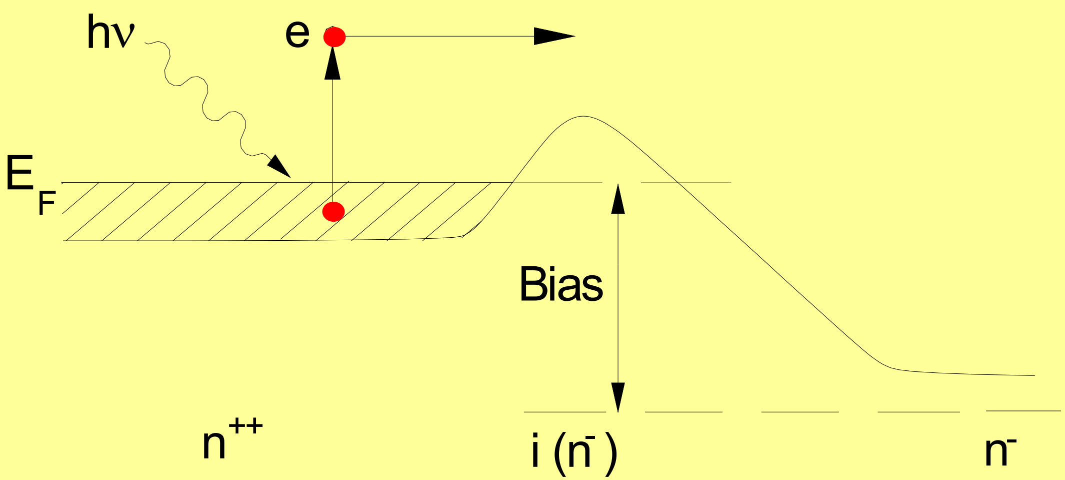

- Fermi level is above the conduction band edge of the barrier
- Conduction band edge of the Emitter and the barrier become degenerate
- Space charge region at the n^{++} - i interface forms the barrier
- Barrier height depends on the concentration and the applied field

JAP **(77)** 915 (1995)

HIWIP/HEIWIP Dual Band Detectors

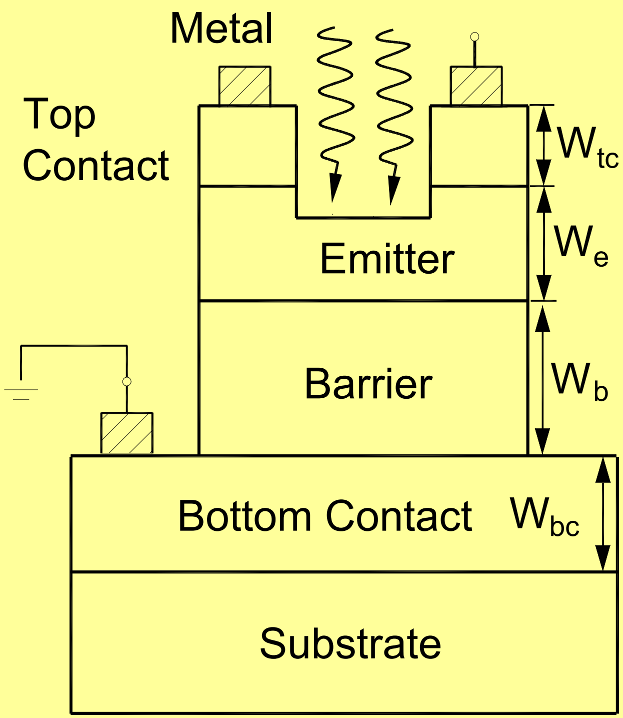

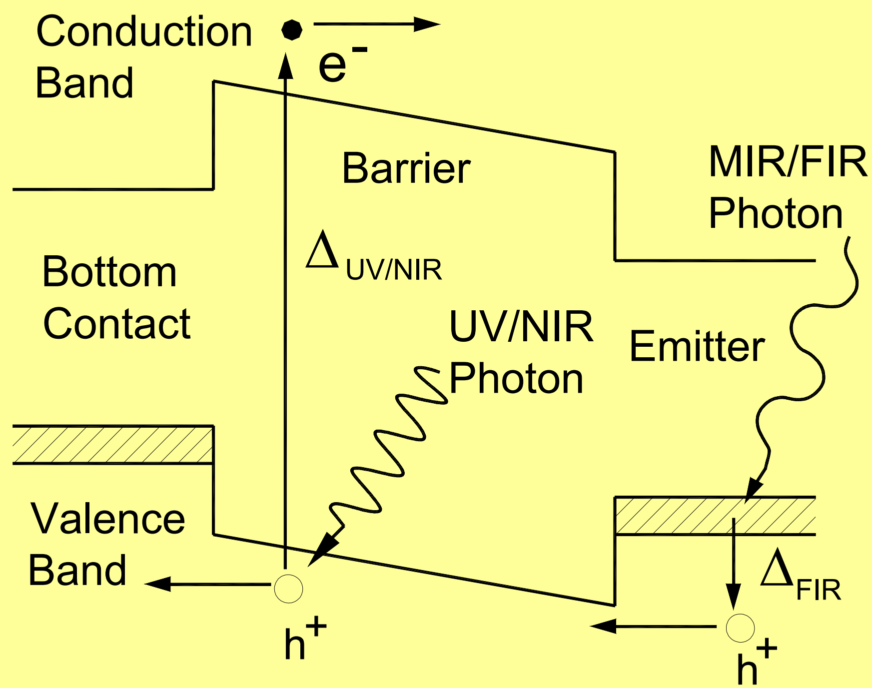

Material Systems

Interband Response >>

InN	0.62 µm (VIS)
GaN	0.39 µm (UV/VIS)
AlN	0.2 µm (UV)
InP	0.93 µm (VIS/NIR)
GaP	0.55 µm (VIS)
InAs	3.50 µm (NIR)
GaAs	0.87 µm (NIR)
AlAs	0.56 µm (VIS)
InSb	7.3 µm (MIR)
GaSb	1.71 µm (NIR)

Intraband Response >> With corresponding emitter material, doping concentration, and the alloy fraction, the wavelength threshold of the intraband (IR) response can be varied.

Si-HIWIP Dual Band Detectors

(OMCVD Grown)

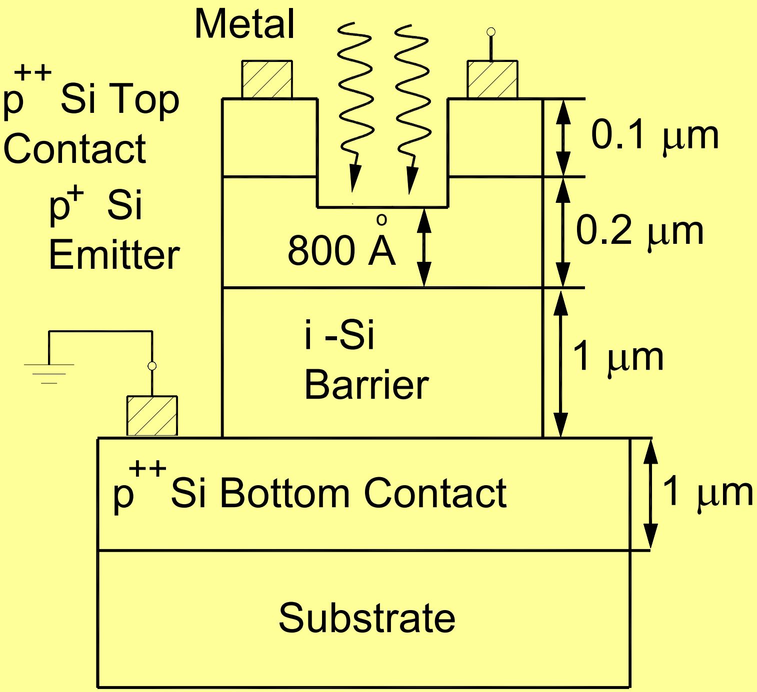

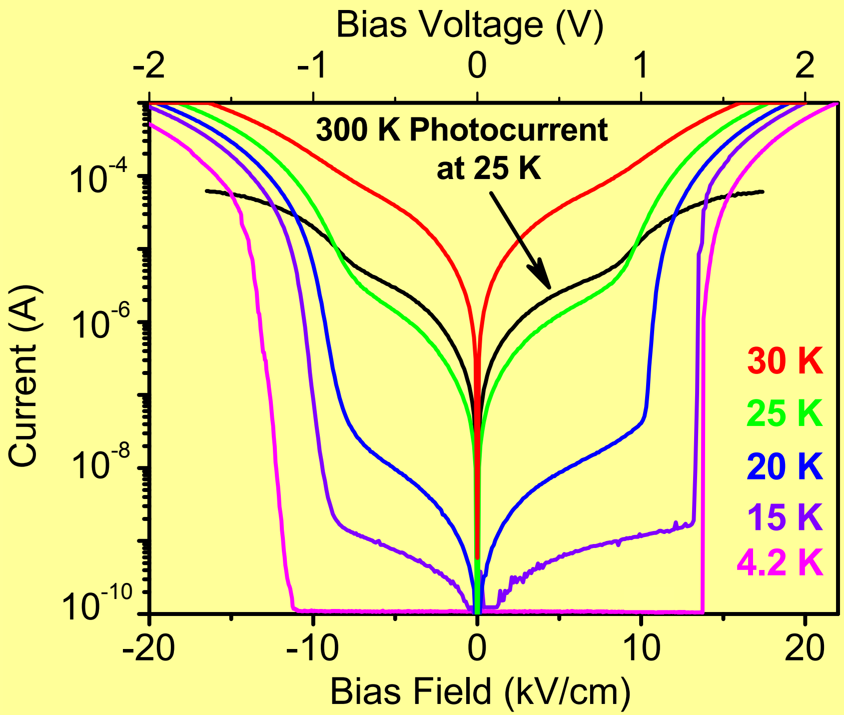

Contact doping = 1.5×10^{19} cm^{-3}

Emitter doping = 2.5×10^{18} cm^{-3}

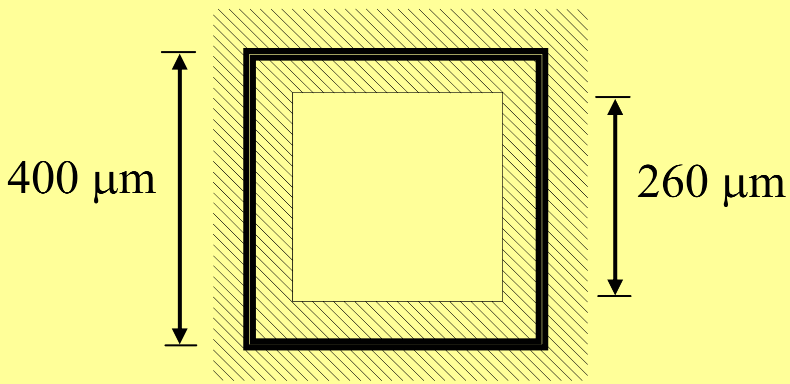

Si-HIWIP VLWIR Response

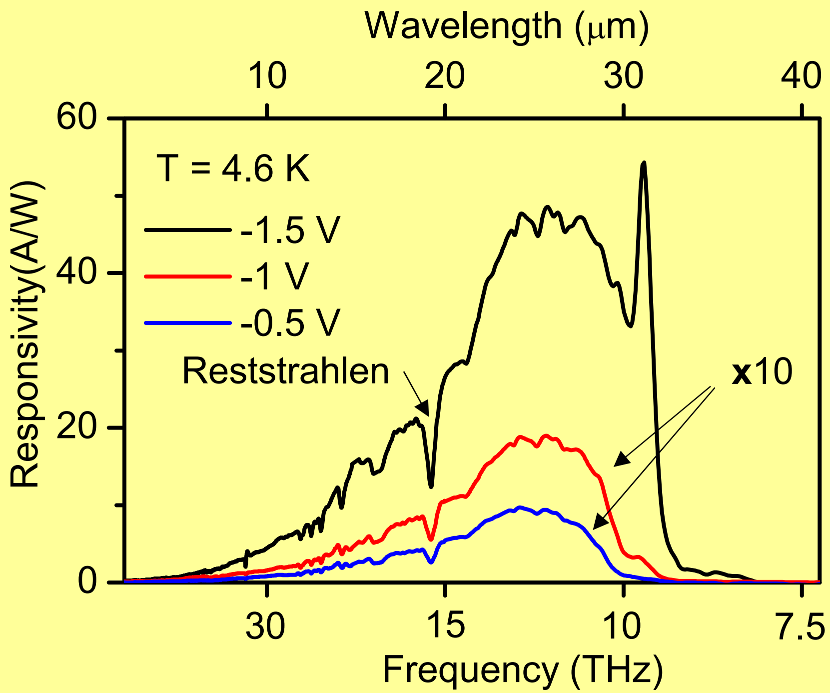

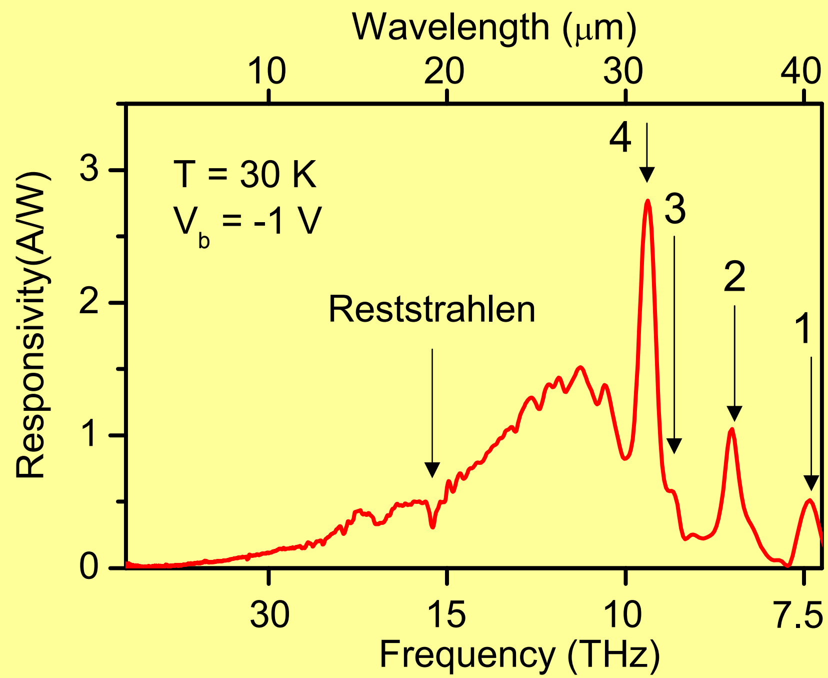

	Boron Impurity Peaks		
	Observed		**Reported by Merlet *et al***
Peak	**(μm)**	**(meV)**	**(meV)**
1	40.4	30.7	30.37
2	36.0	34.4	34.50
3	32.4	38.3	38.38
4	31.3	39.6	39.63

Phy. Rev. (B) **12** 3297(1974)

Si-HIWIP Response under High Fields

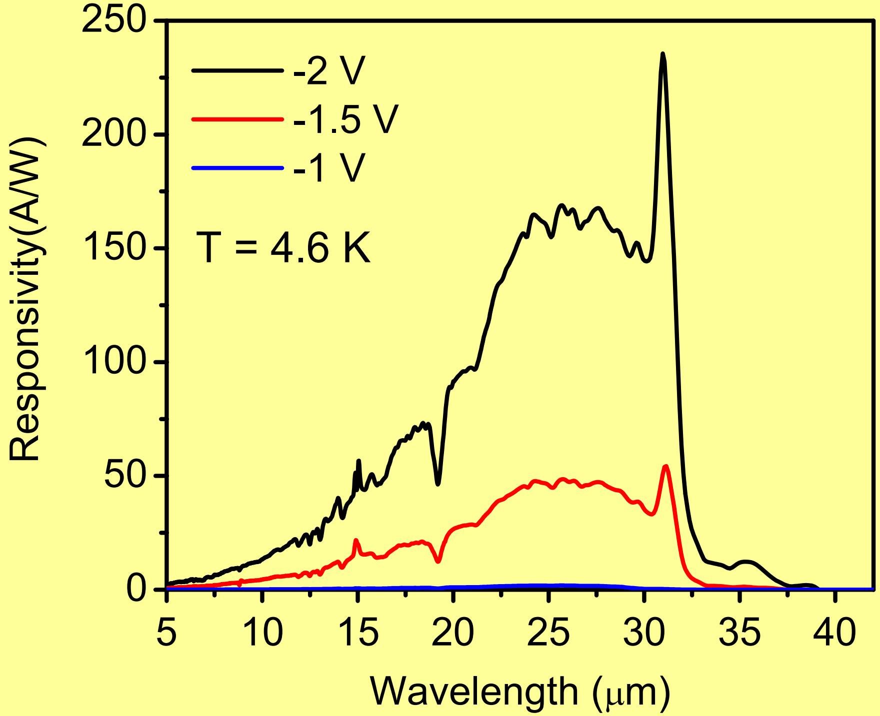

Bias Voltage (V)	(Quantum Efficiency) X (Gain)
-2	5.4
-1.5	1.5
-1	0.05

Si- Dual Band Response

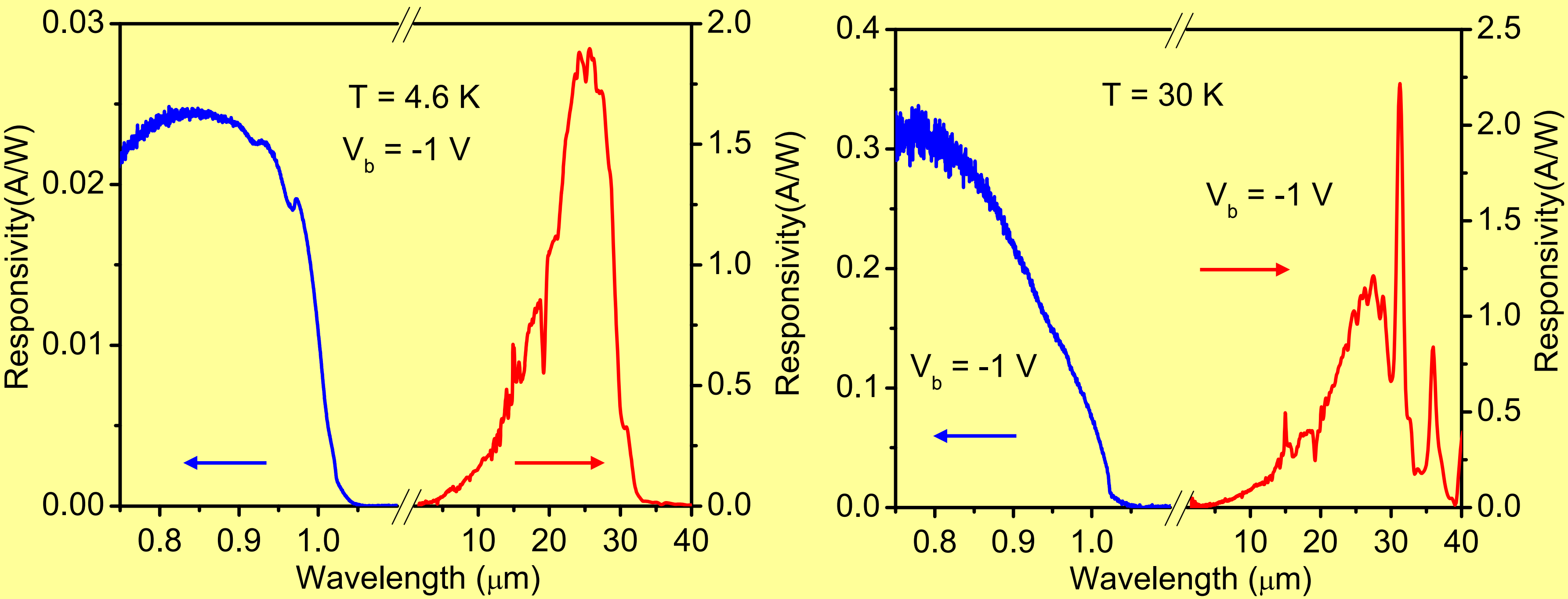

- The sharp peaks at ~ 31.3, 32.4, 36.0, and 40.4 μm correspond to the impurity transitions of Boron in Si.

Comparison with Si : BIB

Si-HIWIP

(Frequency =11 THz)

T (K)	Field (kV/cm)	Wavelength (μm)	Responsivity (A/W)	NEP ($W/Hz^{1/2}$)	D* (Jones)
4.6	-10	10-35	1.7	3.4×10^{-13}	1.2×10^{11}
4.6	-15	10-35	47	4.2×10^{-12}	9.4×10^{9}
4.6	-20	10-35	168	1.4×10^{-11}	2.8×10^{9}
30	-10	10-35	1.4	1.3×10^{-11}	3.1×10^{9}

Si-BIB

T (K)	Wavelength Range (μm)	Responsivity (A/W)	NEP ($W/Hz^{1/2}$)
4.2	5-30	2	
7	2-40	32	1.2×10^{-15}

[1]IR Labs Inc.

[2]Huffman et al. J. Appl. Phys. 273, **72** (1992)

GaAs-HIWIP Dual Band Detector

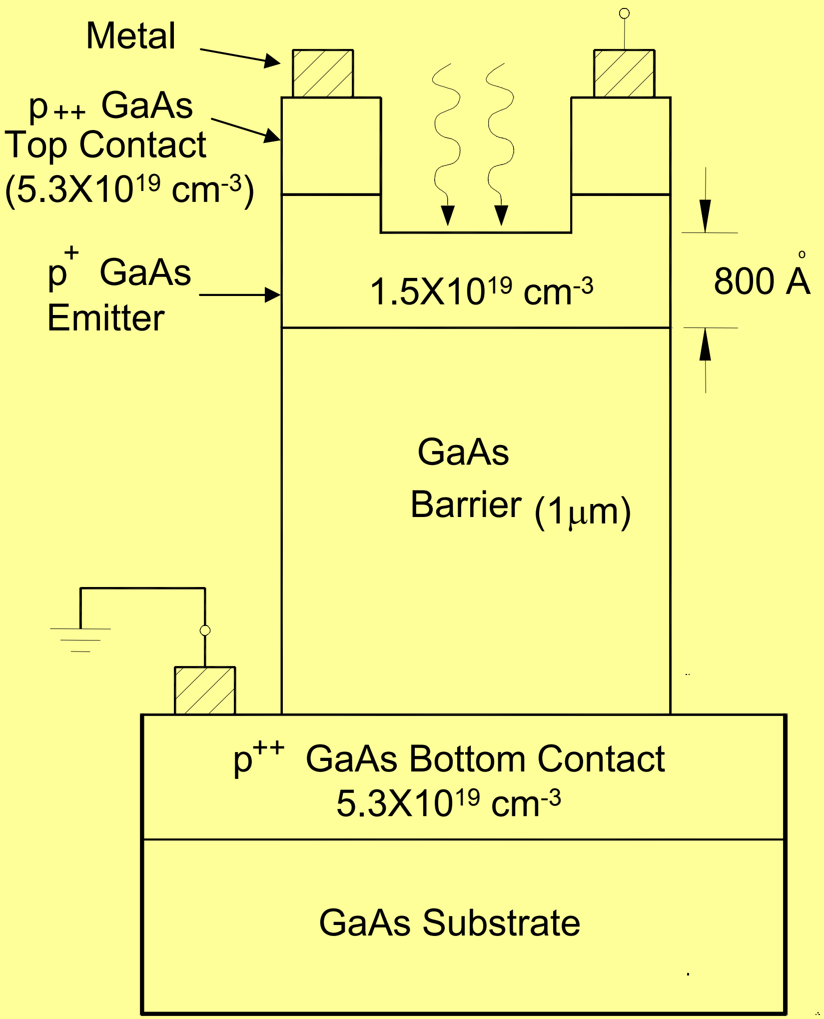

JAP (**96**) 4588 (2004)

- grown by MOCVD technique.
- The emitter is C- doped to $1.5X10^{19}$ cm^{-3}.
- The contact layers are highly doped.

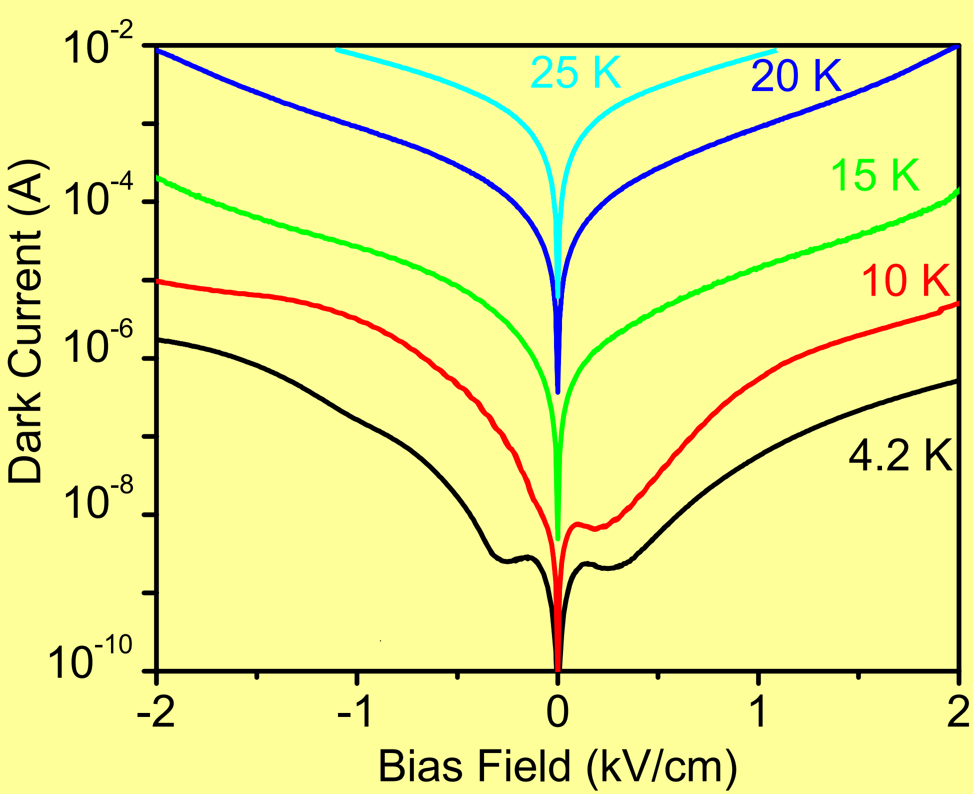

GaAs- Interband Response

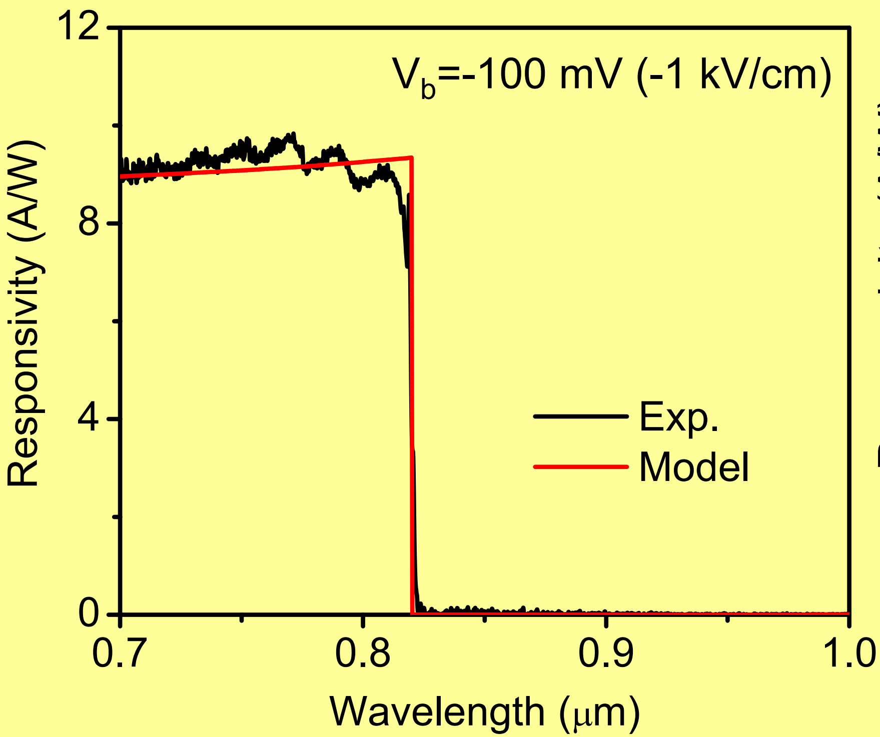

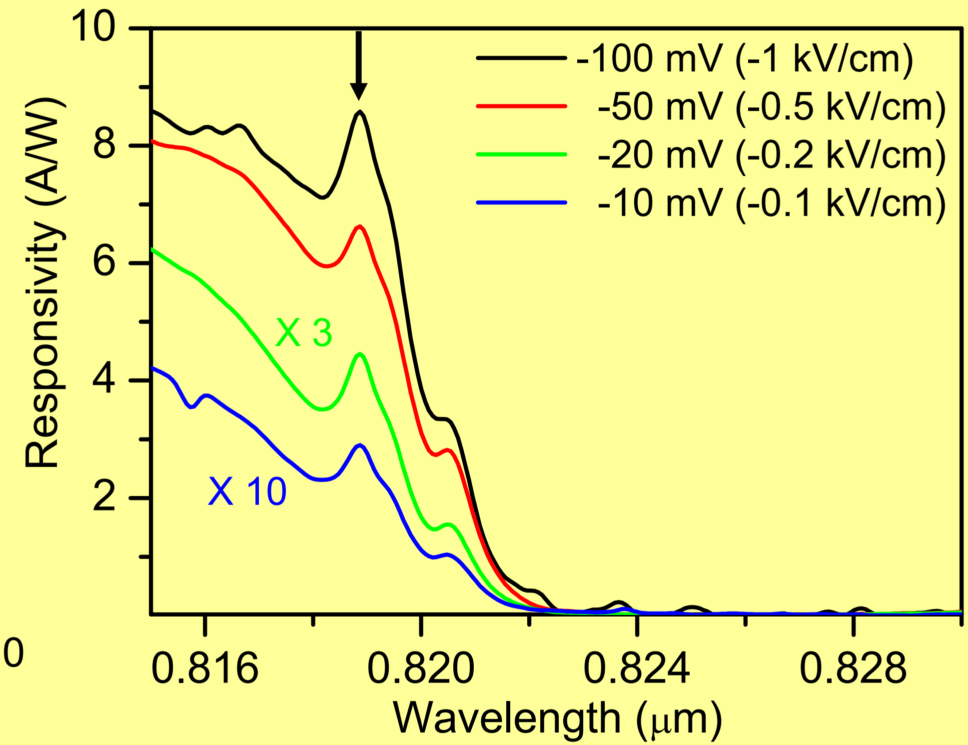

- Sharp drop at ~0.82 μm → band gap in GaAs (1.51 eV @ 4.2 K)
- The arrow at ~0.819 μm indicates an exiton

GaAs- Dual Band Response

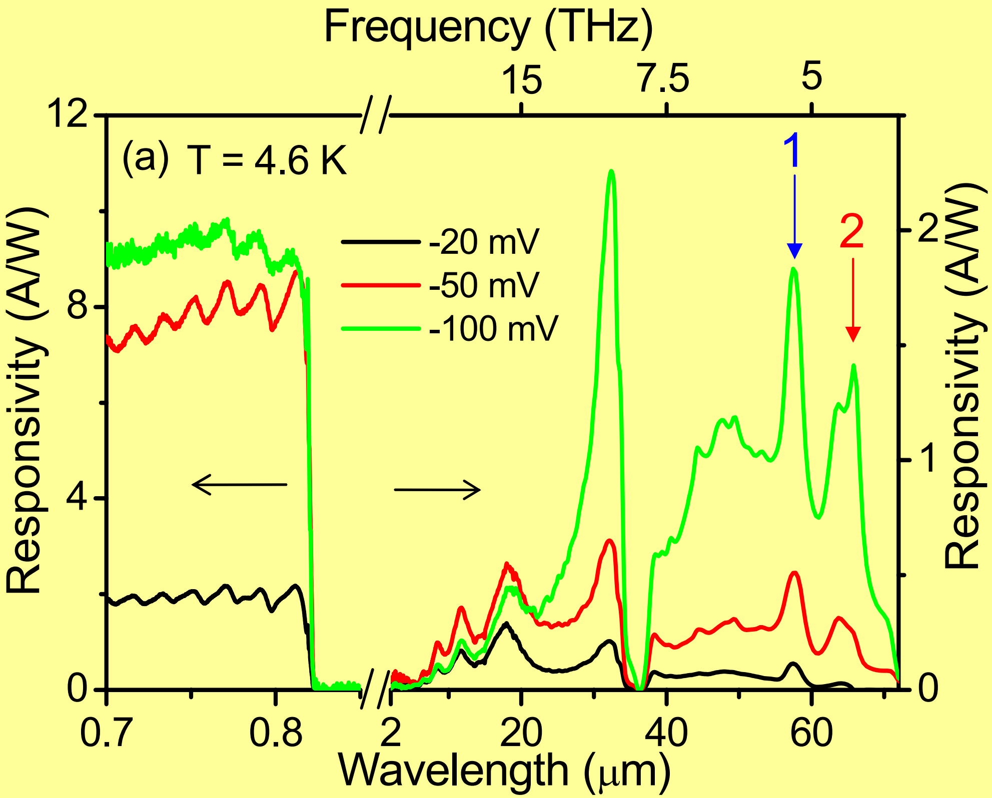

1: $1S_{3/2}(\Gamma_8) \rightarrow 2P_{5/2}(\Gamma_7)$

2: $1S_{3/2}(\Gamma_8) \rightarrow 2P_{5/2}(\Gamma_8)$

- The deep valley around 37 μm is due to TO-Phonon of GaAs.
- The oscillations in MIR region match Fabri-Perot interference in the GaAs layer.

APL(**86**) 143510 (2005)

Impurity Levels J. Phys. C (**11**) 419 (1978)

GaAs- Dual Band Response

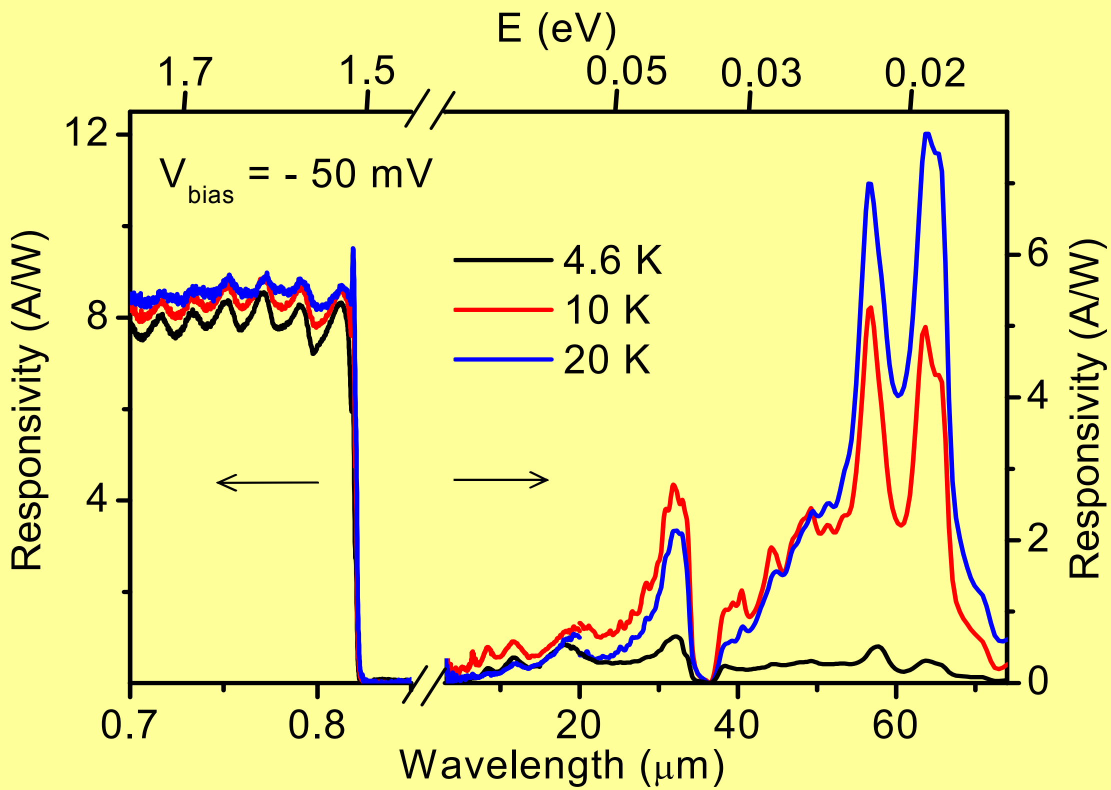

APL(**86**) 143510 (2005)

Advantages of GaN

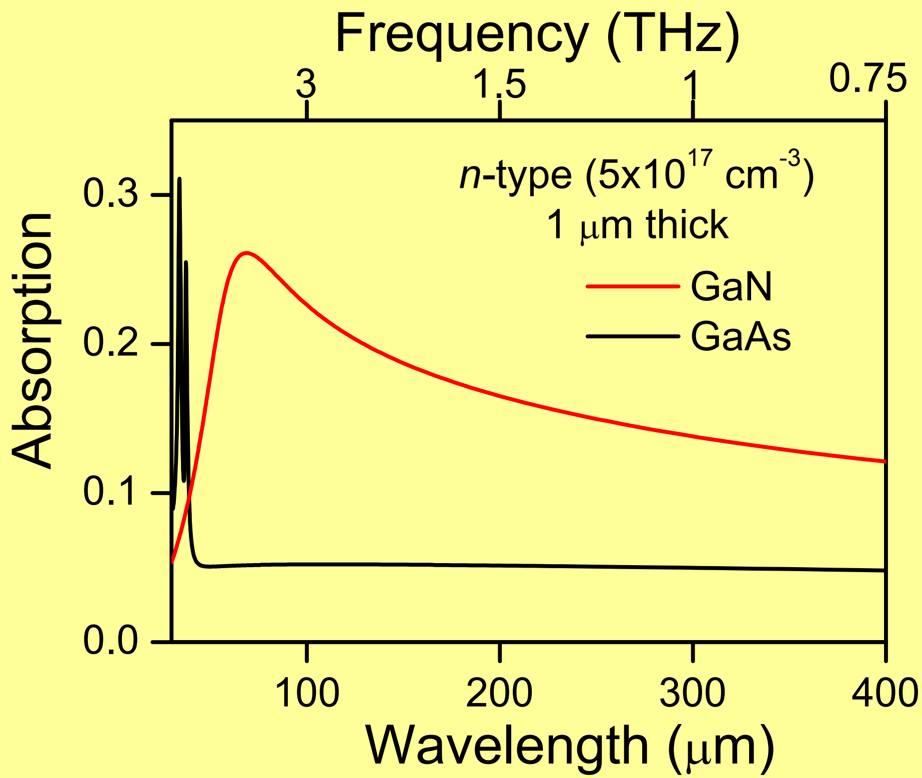

- Higher absorption
- Radiation hard

GaN/AlGaN HEIWIP UV-IR Dual Band Detector

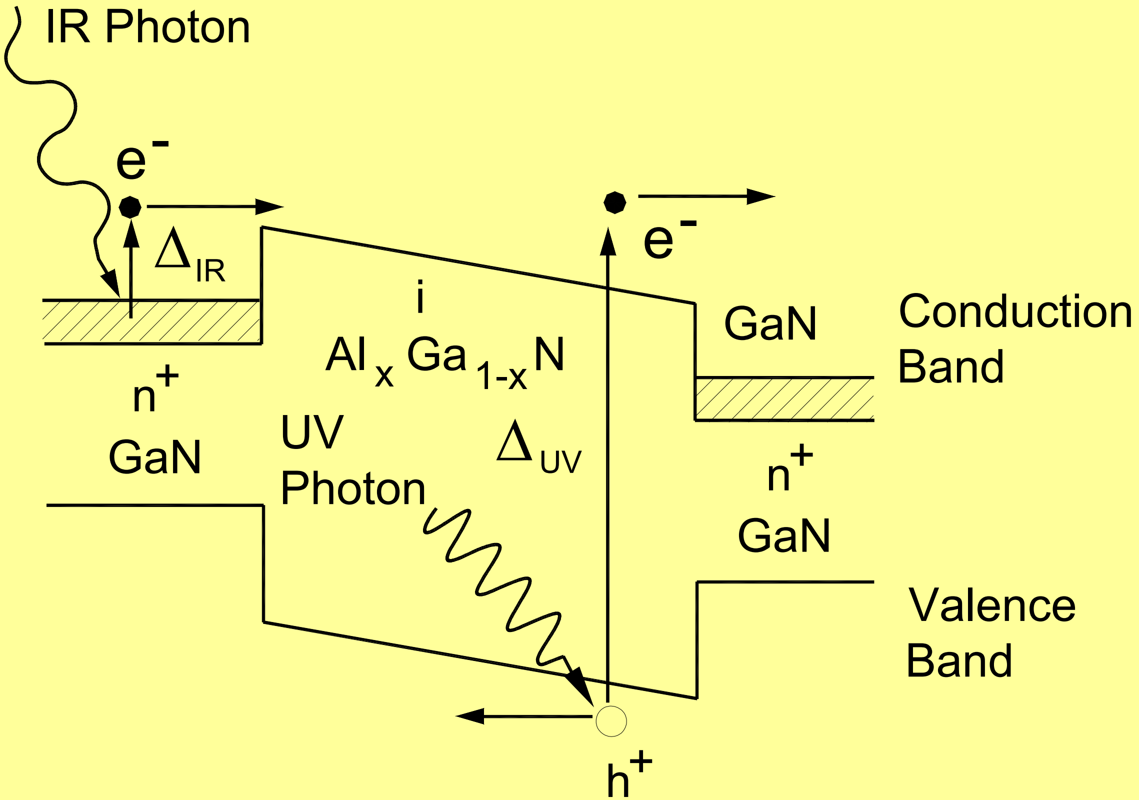

For all AlGaN structure

- Changing the Al fraction in both emitter and barrier by the same amount will change only the interband (UV) threshold.
- Changing the Al fraction only in the emitter will change only the intraband (IR) threshold.

GaN/AlGaN Dual Band Detector Structures

Sample: 1158

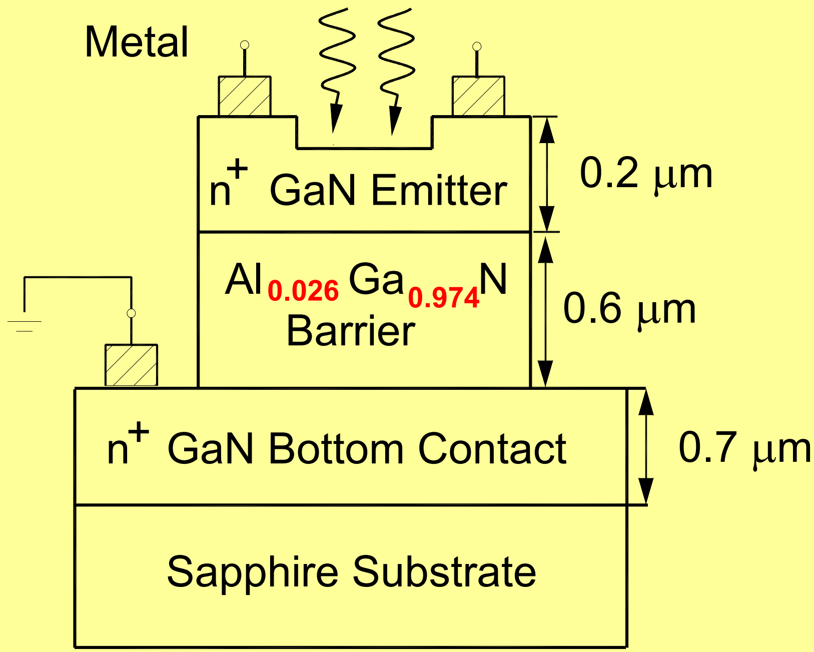

Sample: 1547

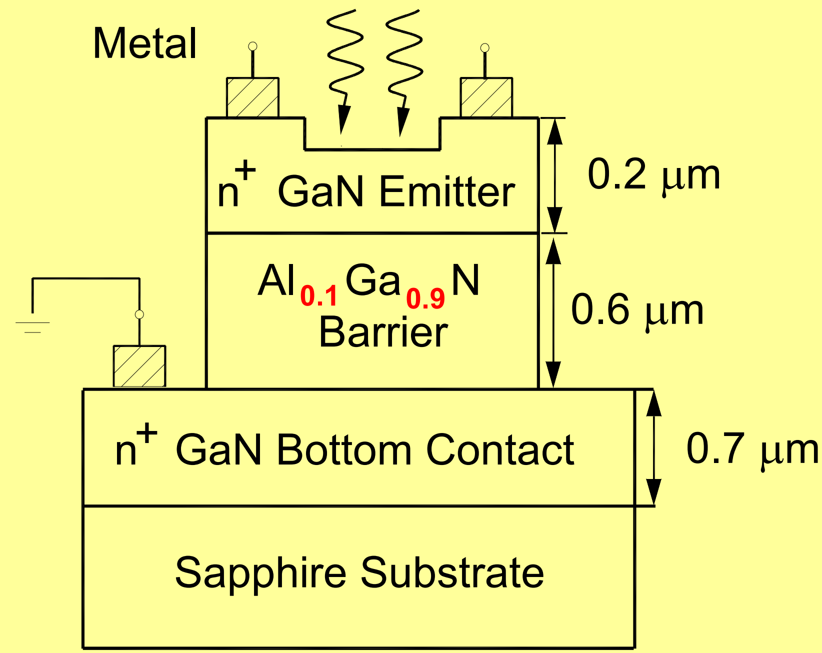

- Different Al fractions in the barrier will change both the interband (uv) and intraband (IR) thresholds.

GaN/AlGaN UV Response

Sample: 1158

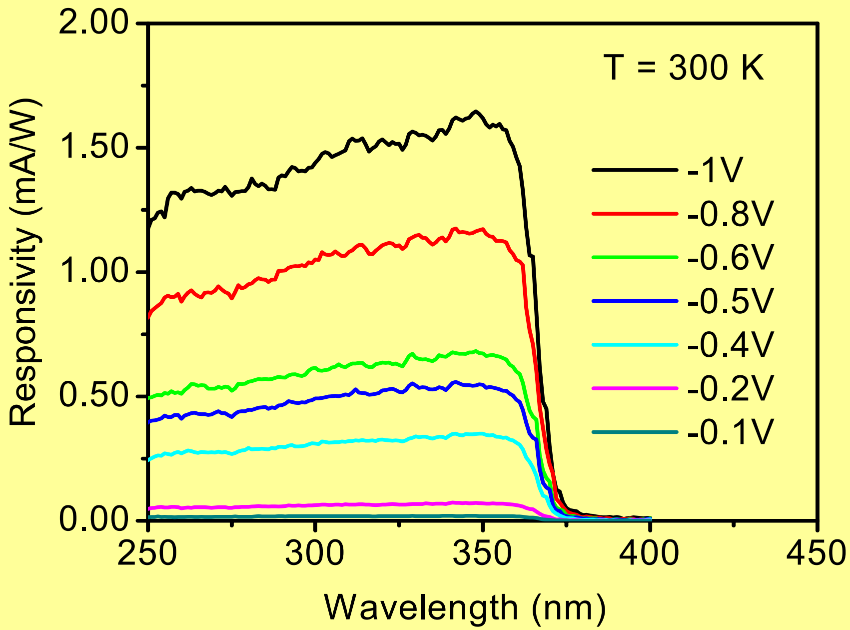

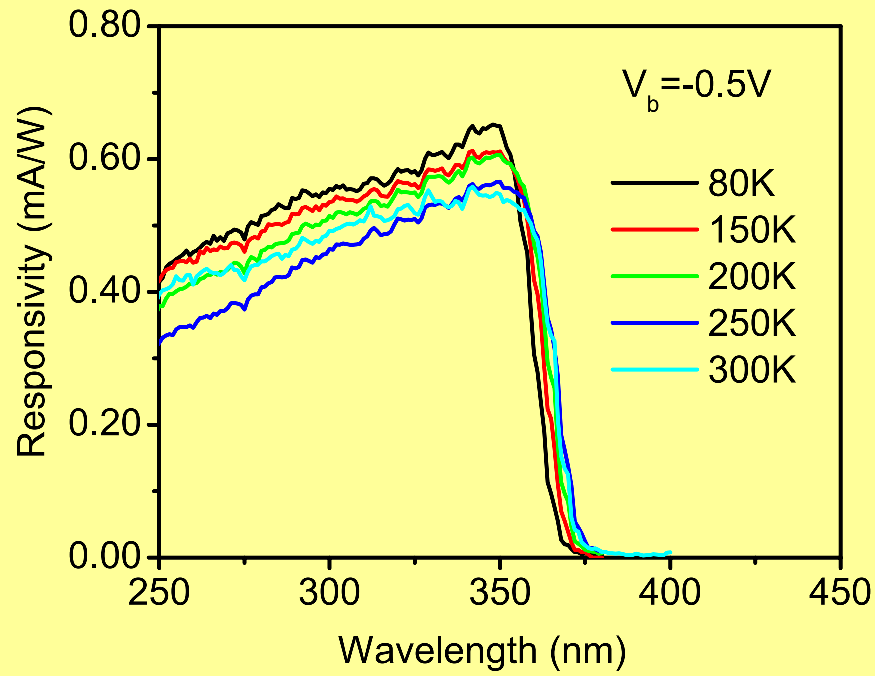

GaN/AlGaN IR Response- Sample 1158

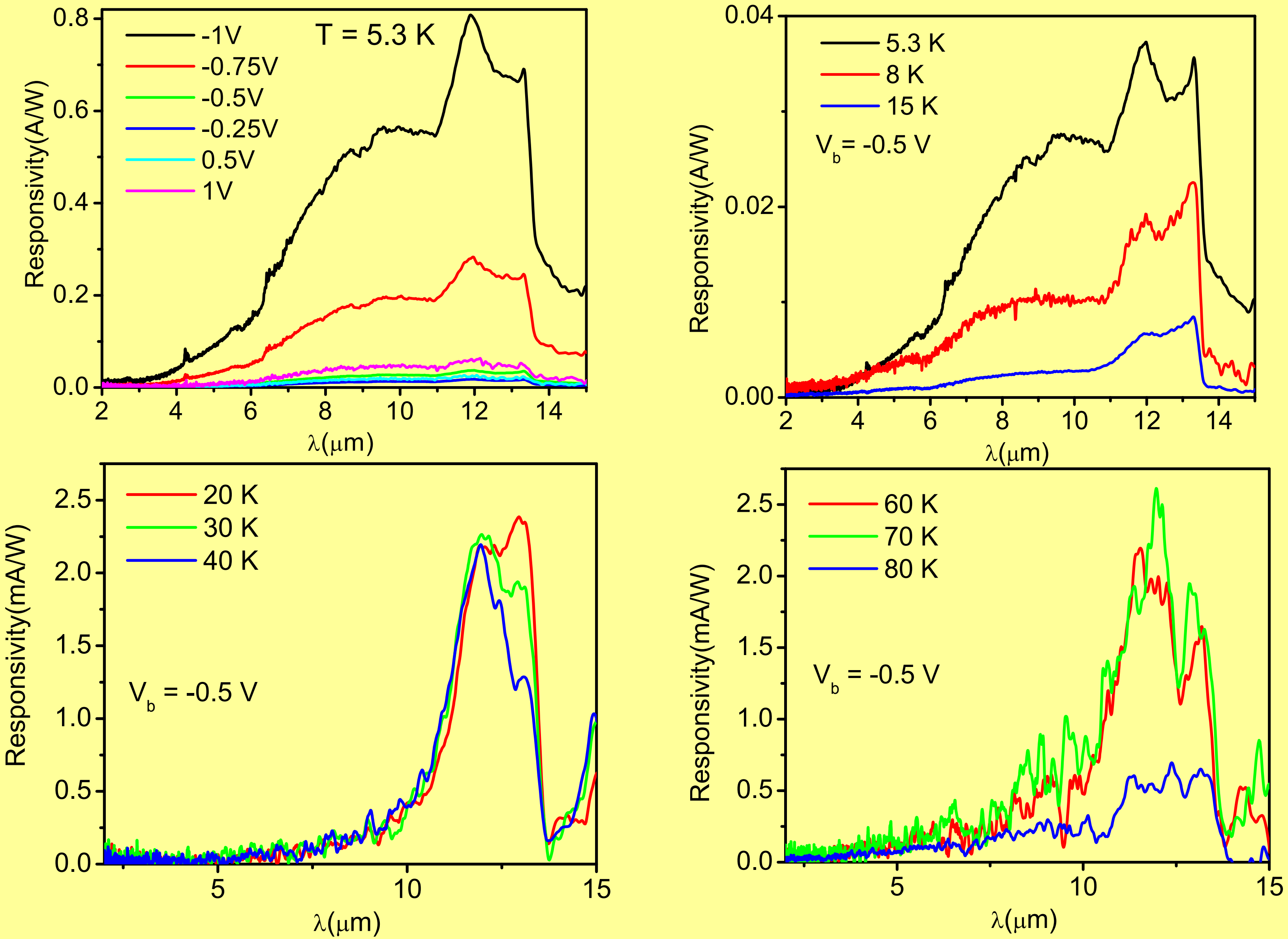

GaN/AlGaN Dual Band Response- Sample 1158

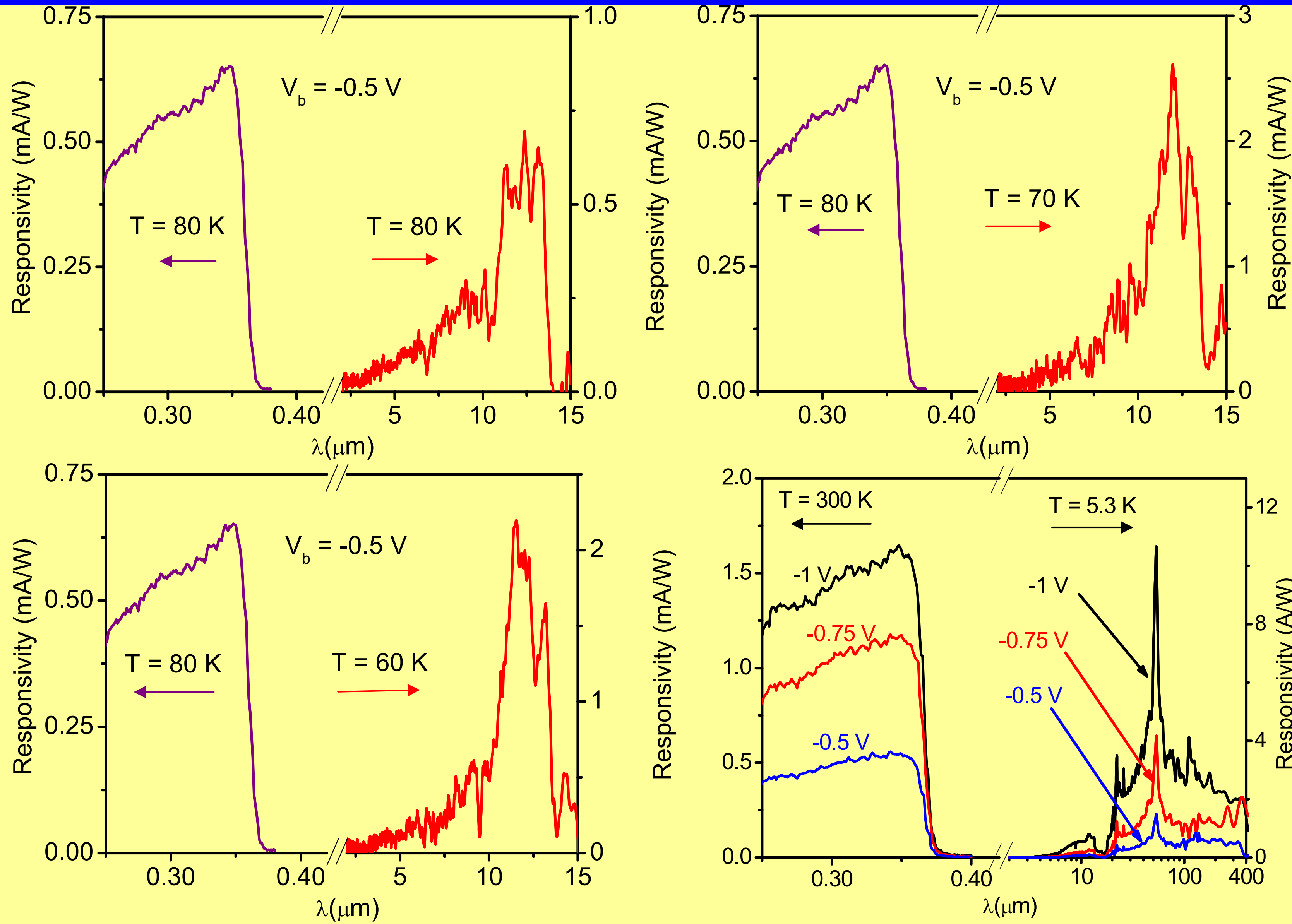

GaN/AlGaN Dual Band Response

Sample: 1158

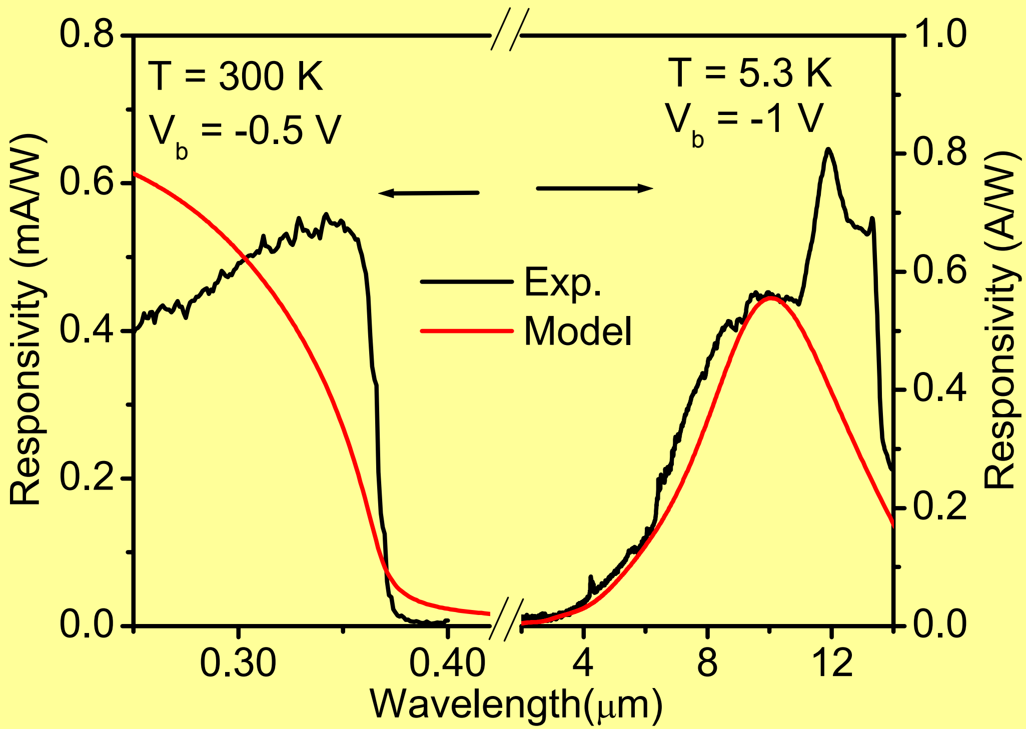

UV Model: J. Appl. Phys. (**82**) 3528 (1997)

GaN/AlGaN Dual Band Response

Sample: 1547

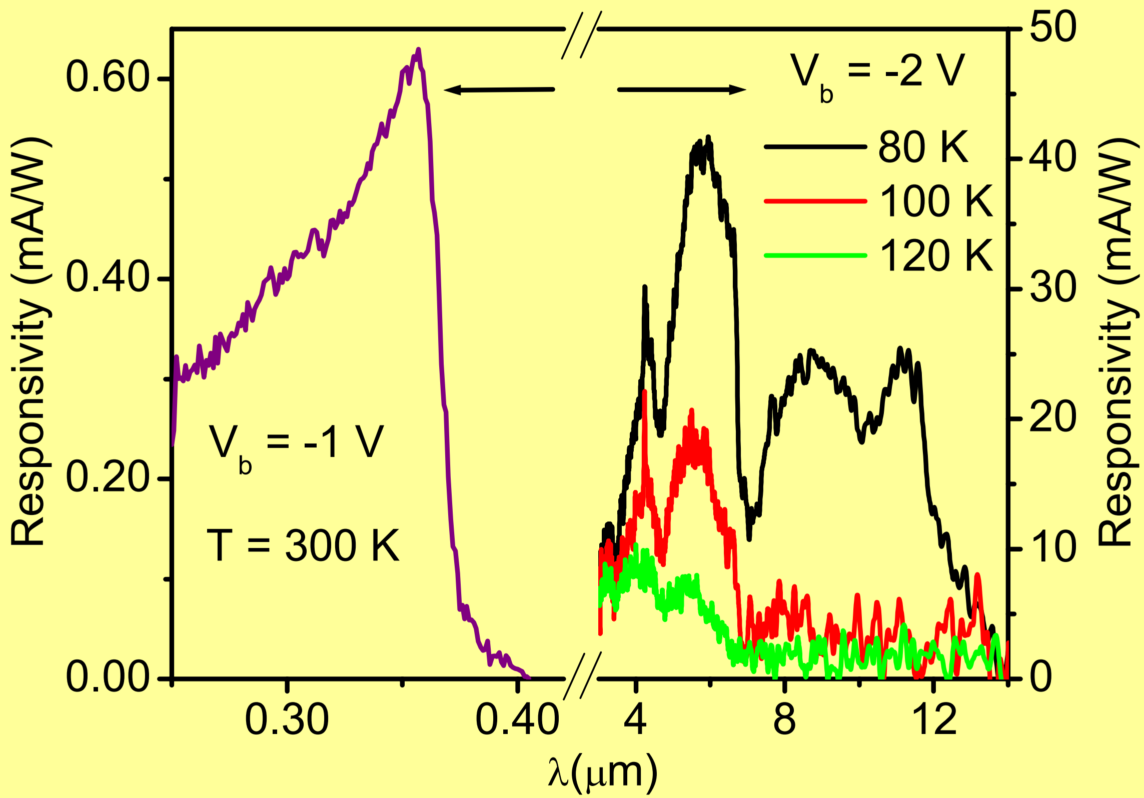

GaN/AlGaN Dual Band Response

Sample: 1547

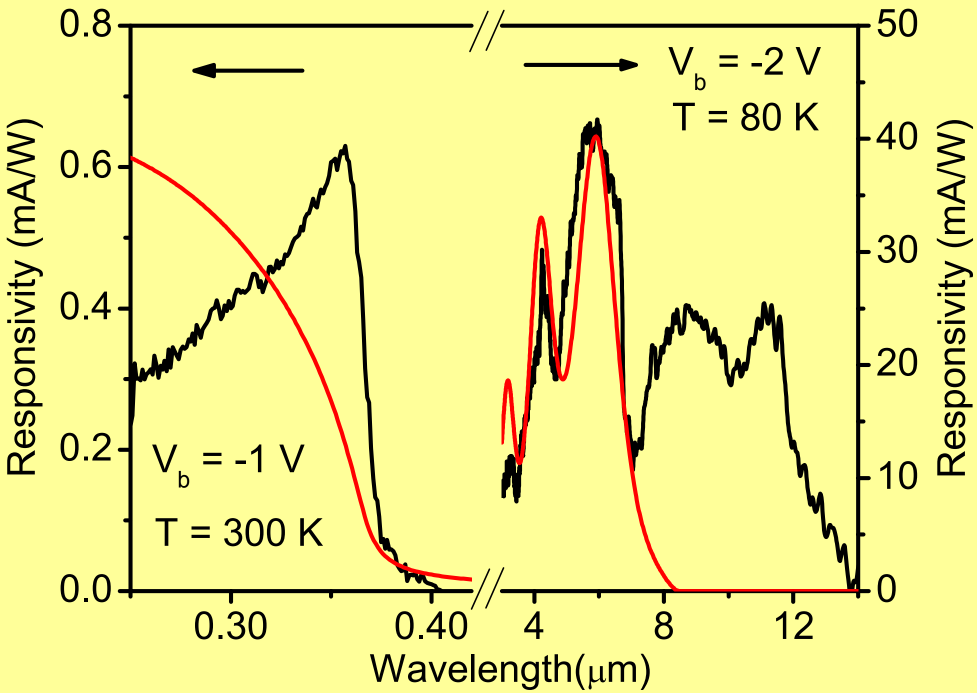

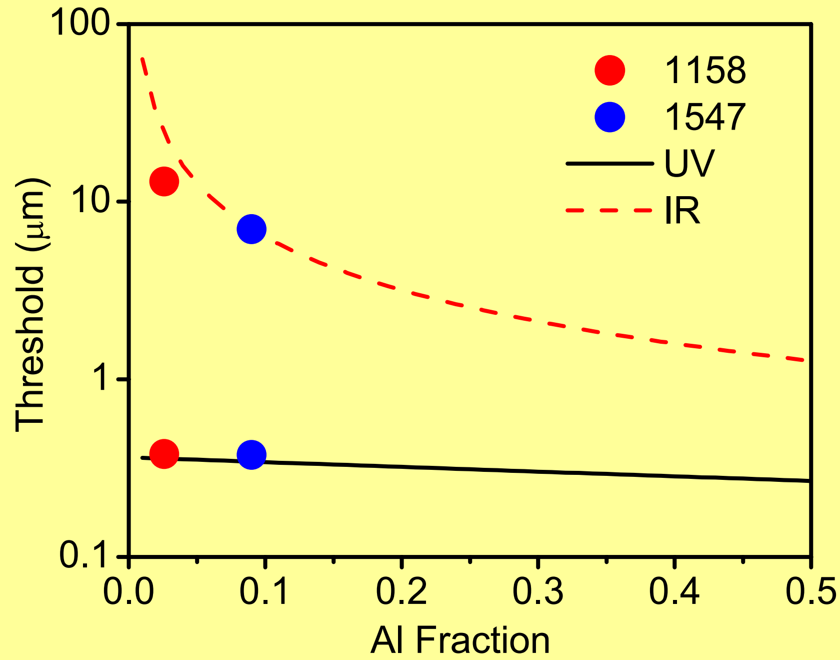

GaN/AlGaN THz Response

Sample: 1158

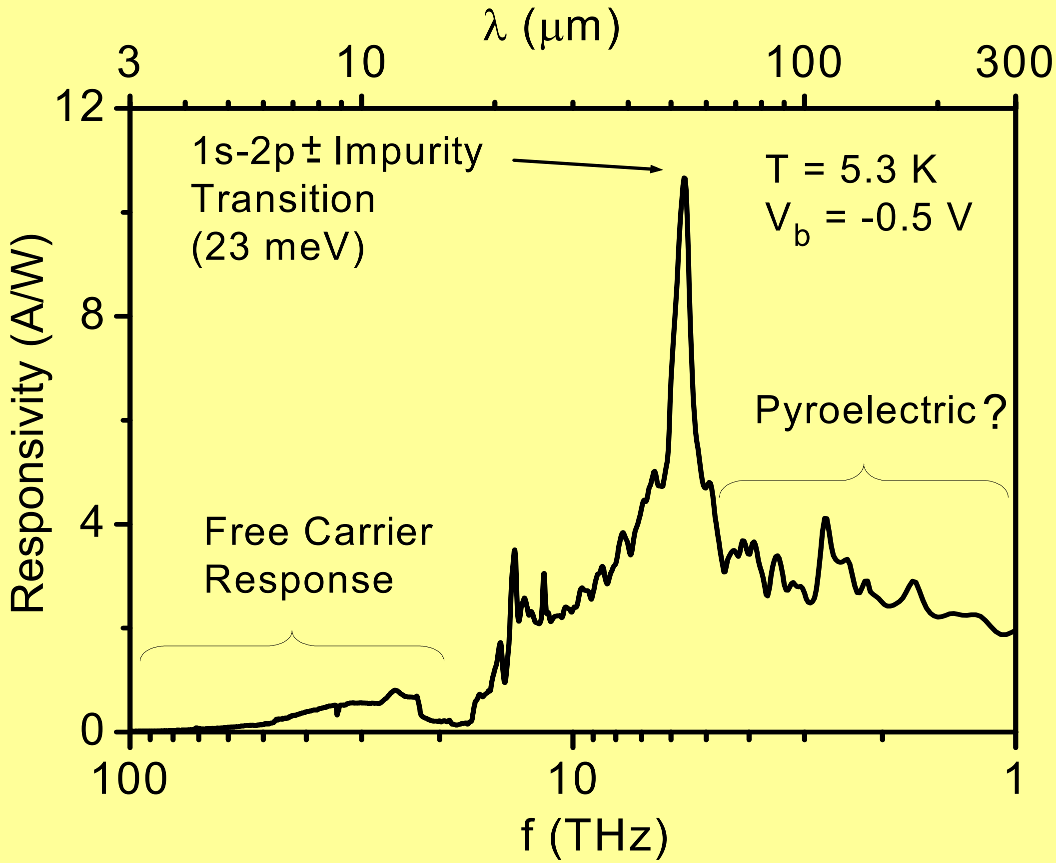

Conclusion

- HIWIP GaAs - NIR/VLIR Dual Band Response

  Si - NIR/VLIR Dual Band Response

- HEIWIP GaN material high absorption

  UV/ IR Dual Band Resposne

  Changing Al fraction in GaN/AlGaN HEIWIP detectors

  changes either UV or IR, or both thresholds.